Journal of Muscle Research and Cell Motility **23**: 483–497, 2002.

Cardiac titin: molecular basis of elasticity and cellular contribution to elastic and viscous stiffness components in myocardium

WOLFGANG A. LINKE[1,*] and JULIO M. FERNANDEZ[2]
[1]*Institute of Physiology and Pathophysiology, University of Heidelberg, Im Neuenheimer Feld 326, D-69120 Heidelberg, Germany;* [2]*Department of Biological Sciences, Columbia University, New York, NY, USA*

Abstract

Myocardium resists the inflow of blood during diastole through stretch-dependent generation of passive tension. Earlier we proposed that this tension is mainly due to collagen stiffness at degrees of stretch corresponding to sarcomere lengths (SLS) ≥2.2 μm, but at shorter lengths, is principally determined by the giant sarcomere protein titin. Myocardial passive force consists of stretch-velocity-sensitive (viscous/viscoelastic) and velocity-insensitive (elastic) components; these force components are seen also in isolated cardiac myofibrils or skinned cells devoid of collagen. Here we examine the cellular/myofibrillar origins of passive force and describe the contribution of titin, or interactions involving titin, to individual passive-force components. We construct force–extension relationships for the four distinct elastic regions of cardiac titin, using results of *in situ* titin segment-extension studies and force measurements on isolated cardiac myofibrils. Then, we compare these relationships with those calculated for each region with the wormlike-chain (WLC) model of entropic polymer elasticity. Parameters used in the WLC calculations were determined experimentally by single-molecule atomic force-microscopy measurements on engineered titin domains. The WLC modelling faithfully predicts the steady-state-force *vs.* extension behavior of all cardiac-titin segments over much of the physiological SL range. Thus, the elastic-force component of cardiac myofibrils can be described in terms of the entropic-spring properties of titin segments. In contrast, entropic elasticity cannot account for the passive-force decay of cardiac myofibrils following quick stretch (stress relaxation). Instead, slower (viscoelastic) components of stress relaxation could be simulated by using a Monte-Carlo approach, in which unfolding of a few immunoglobulin domains per titin molecule explains the force decay. Fast components of stress relaxation (viscous drag) result mainly from interaction between actin and titin filaments; actin extraction of cardiac sarcomeres by gelsolin immediately suppressed the quickly decaying force transients. The combined results reveal the sources of velocity sensitive and insensitive force components of cardiomyofibrils stretched in diastole.

Introduction

A wealth of information collected over the past decade has provided us with exciting new insight in the elasticity of titin (initially described as connectin; Maruyama *et al.*, 1977), the giant muscle protein (Wang, 1996; Trinick and Tskhovrebova, 1999). Among the well-known 'stretchy' biomolecules (Alper, 2002) – many of which are covered in this issue – titin arguably still is a 'newcomer', considering that its amino-acid sequence was elucidated only some 7 years ago (Labeit and Kolmerer, 1995). However, within a relatively short time, the concerted efforts of several research groups have led to a mechanical characterization of titin in such a detail that by now it can be said that the molecular mechanisms of titin elasticity are no secret anymore. The importance of a detailed understanding of titin mechanics is illuminated by the fact that changes in the elastic function of cardiac-titin regions accompany severe heart failure in humans (Neagoe *et al.*, 2002). In myocardium, titin acts together with collagen to determine the passive tension (PT) of the ventricular wall during diastolic filling. A brief update of an earlier report discussing the role of titin and collagen in cardiac muscle (Linke *et al.*, 1994) is provided here (Figure 1).

Titin is a ≥1 μm long and slender protein of 3–3.7 MDa size (Labeit and Kolmerer, 1995) that is present in all sarcomeres. A titin molecule extends over half of a sarcomere from the Z-disk to the M-line (cf., Figure 2A; Fürst *et al.*, 1988; Itoh *et al.*, 1988). Only the I-band titin is functionally elastic (except a 100-nm-wide region on either side of the Z-disk, which is tightly associated with the thin filaments; Linke *et al.*, 1997; Trombitas *et al.*, 1997). Like A-band titin (Labeit *et al.*, 1992), the elastic I-band titin region is assembled in a modular fashion (Figure 2A). Many individually folded domains of the immunoglobulin (Ig) type (Politou *et al.*, 1995; Improta *et al.*, 1996) are interspersed with unique sequences (Labeit and Kolmerer, 1995). The composition of I-band titin is regulated by alternative splicing,

*To whom correspondence should be addressed: Tel.: +49-6221-544130; Fax: +49-6221-544049; E-mail: wolfgang.linke@urz.uni-heidelberg.de

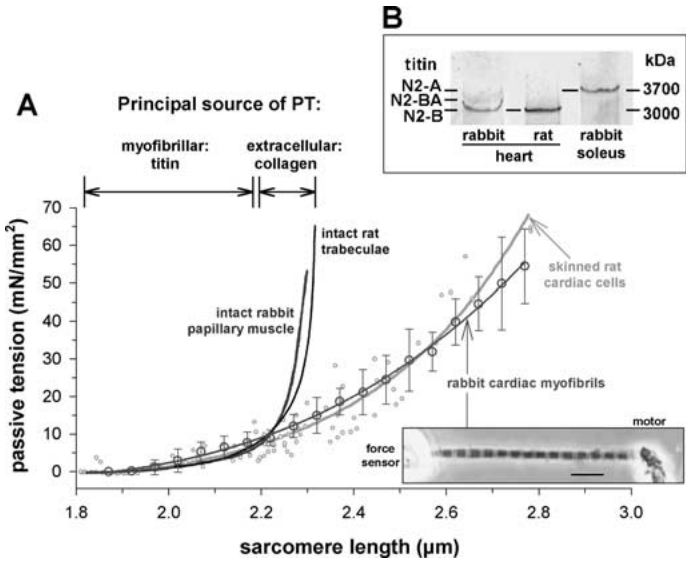

Fig. 1. Sources of PT in various cardiac-muscle preparations stretched under relaxing conditions. (A) Comparison of passive SL–tension curves of intact rabbit (Julian *et al.*, 1976) and intact rat (Kentish *et al.*, 1986) cardiac fibers with those of skinned rat cardiomyocytes (small grey symbols; Weiwad *et al.*, 2000) and isolated rabbit cardiac myofibrils (large symbols and error bars; Linke, 2000). Arrows in upper left corner indicate which protein dominates PT development in the left ventricle at which SL (Linke *et al.*, 1994). (B) 2% SDS–polyacrylamide gel to detect titin isoforms (for methodological description, cf., Neagoe *et al.*, 2002). Both rabbit and rat heart express almost exclusively N2B-titin. Rabbit soleus-titin band (N2A-titin isoform) is shown for comparison.

giving rise to muscle type-specific isoforms (Freiburg *et al.*, 2000). The titin isoform with the shortest I-band region is found in cardiac-muscle sarcomeres (N2B-isoform) and has a molecular mass of 2970 kD (Labeit and Kolmerer, 1995). This N2B-isoform makes up ~70% of all titin isoforms in normal human left ventricle, the remainder being various isoforms of a so-called N2BA type (Neagoe *et al.*, 2002). The elastic I-band region of N2B-titin can be subdivided into four structurally distinct regions (Figure 2): (1) a proximal Ig region containing 15 tandem-Ig domains; (2) a middle N2-B segment that contains a 572-residue amino-acid sequence of unknown structure; (3) a 186 amino-acid-long segment rich in proline (P), glutamate (E), valine (V) and lysine (K) residues, named the PEVK region; and (4) a distal Ig region containing 22 Ig-domain repeats. Whereas the middle N2-B segment is specific to titin in cardiac muscle, alternatively spliced isoforms of titin in other muscle tissues add varying numbers of Ig modules to the proximal Ig region and additional residues to the PEVK domain (Freiburg *et al.*, 2000). For example, human soleus titin (a so-called N2A-isoform, like in all skeletal muscles) contains an additional 53 proximal Ig domains and a PEVK region of 2174 residues (Labeit and Kolmerer, 1995). Thus, by adjusting the length of titin's extensible region, a muscle can vary its elastic properties (Linke *et al.*, 1996b).

Thanks to a combination of two novel approaches, protein engineering and single-molecule force spectroscopy using the atomic force microscope (AFM) (Carrion-Vazquez *et al.*, 2000), we can now study the contribution of the individual building blocks of titin, one by one, to the protein's overall elasticity (Li *et al.*, 2002). A complex mechanical behavior of cardiac titin is apparent, which originates in the structural heterogeneity of this finely tuned molecular spring. In this study, we investigate how the force–extension relationships of the four distinct N2B cardiac-titin regions measured *in situ* (Linke *et al.*, 1999) compare to those calculated with the wormlike-chain (WLC) model of entropic polymer elasticity, which has been successfully applied to explain the elastic behavior of single titin molecules (Kellermayer *et al.*, 1997; Rief *et al.*, 1997; Tskhovrebova *et al.*, 1997). Importantly, the parameters established by AFM mechanics on engineered titin domains (Li *et al.*, 2002) could be used to feed the WLC model. This way we probed the idea that entropic (WLC-like) elasticity of the individual titin segments underlies the elastic behavior of whole cardiac I-band titin.

Another aspect is that cardiac muscle works under nonequilibrium conditions – mammalian heart is stretched (and released) one or many times per second. Diastolic force development is not purely elastic, but has long been known to include stretch velocity-sensitive components of viscous and/or viscoelastic nature (Noble, 1977; Chiu *et al.*, 1982; de Tombe and ter Keurs, 1992; Bartoo *et al.*, 1997). The question of how titin might contribute to these force components, was another focus of the present analysis. Specifically, we asked whether titin itself, or interactions involving the elastic titin segment (Kulke *et al.*, 2001a), could play a role for the viscous force decay (stress relaxation) following stretch of cardiac myofibrils. Altogether, we provide a detailed characterization of the molecular events within cardiac myofibrils relevant to the elastic and viscoelastic behavior of myocardium in diastole.

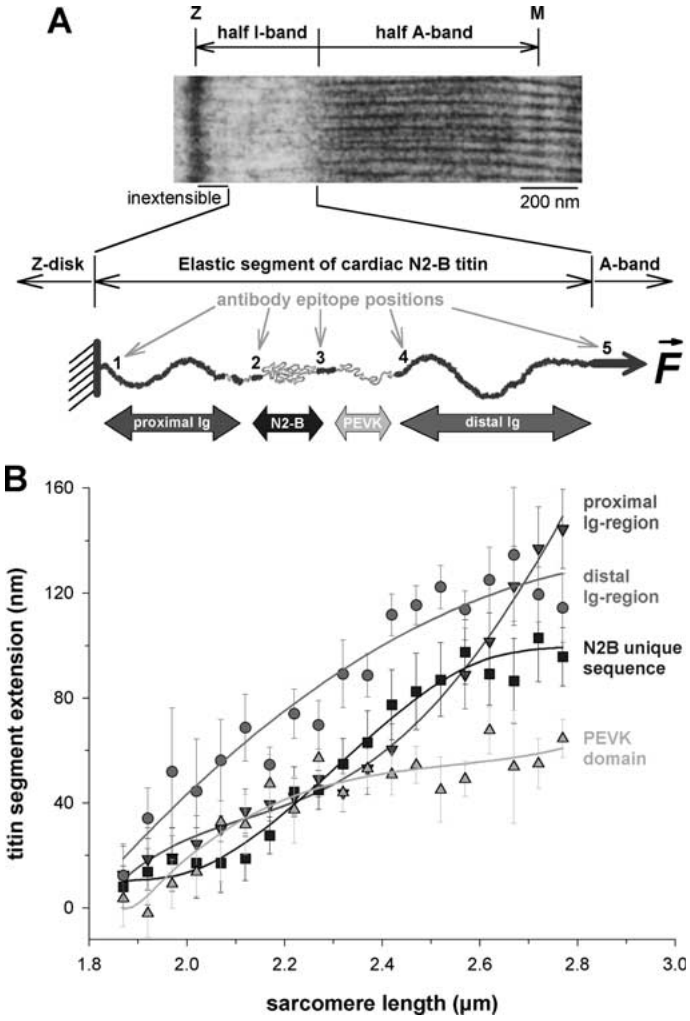

Fig. 2. Extension of cardiac I-band titin (N2B-isoform) *in situ*. (A) Four distinct elastic regions make up the extensible titin segment in each half I-band. Top picture shows electron micrograph of a half-sarcomere. The scheme below also indicates the epitope positions of titin-specific antibodies (1–5) to sites flanking the four elastic regions; these antibodies were used to measure the stretch-dependent extension of titin regions (Linke *et al.*, 1999). (B) Relationship between titin-segment extension and SL, compiled from the original results of immunoelectron/immunofluorescence microscopical analyses of rabbit cardiac sarcomeres (Linke *et al.*, 1999). Symbols show mean ± error estimate; fit curves are third-order regressions.

Materials and methods

Myofibril mechanics

Myofibrils were isolated from freshly excised rabbit cardiac muscle as described (Linke *et al.*, 1996b). Briefly, thin muscle strips were dissected, tied to thin glass rods and skinned in buffer solution ('rigor', composed of (in mM): KCl 75, Tris 10, $MgCl_2$ 2, EGTA 2, pH 7.1) containing 0.5% Triton X-100 for ≥4 h. The skinned strips were minced and homogenized in rigor buffer. All steps were performed at 4°C. A drop of the suspension was placed on a cover slip on the stage of an inverted microscope (Zeiss Axiovert 135). Glass microneedles attached to a piezoelectric micromotor (Physik Instrumente, Waldbrunn, Germany) and a home-built force transducer (sensitivity, ~5 nN, resonant frequency, ~700 Hz), respectively, were used to pick up single myofibrils or small bundles containing 2–4 myofibrils. To firmly anchor the specimen ends, the needle tips were coated with a silicone adhesive in a 1:1 (v/v) mixture of Dow Corning 3145 RTV and 3140 RTV. Water-hydraulic micromanipulators (Narishige, Japan) were used to control the position of both needles. Experiments were performed at room temperature in relaxing solution of 200 mM ionic strength, pH 7.1. Relaxing solution (for composition, see Linke *et al.*, 1997) contained 20 mM 2,3-butanedione monoxime to suppress any, possibly remaining, contractile activity. All solutions were supplemented with the protease inhibitor leupeptin to minimize titin degradation (Linke *et al.*, 1998b). In some experiments, a Ca^{2+}-independent gelsolin fragment (kindly provided by Dr H. Hinssen) was added to the relaxing buffer (final concentration, 0.2 mg/ml) to extract actin (Linke *et al.*, 1997).

Force data collection and motor control were done with a PC, data acquisition (DAQ) board (PCI-MIO-16-E1, National Instruments, Austin, TX) and custom-written LABVIEW software (Linke *et al.*, 1998a, b). Sarcomere length (SL) was measured either with a color

CCD camera (Sony) and frame grabber board including image processing software (Scion Image) or by digitizing and analyzing the myofibril image, using a 2048-element linear photodiode array (Sony), the PC, DAQ board, and LABVIEW algorithms. Force sampling rate typically was 5 kHz. Force data were stored in binary format and were median-filtered off-line. If it was desirable to compare force data from different experiments, the force was related to cross-sectional area inferred from the diameter of the specimens as described (Linke *et al*., 1997).

Analysis of the stretch force-dependent in situ extension of cardiac titin

Immunoelectron and immunofluorescence microscopy with monoclonal or polyclonal antibodies flanking the four distinct regions of the elastic I-band titin (see Figure 2A) was used previously to establish the extensibility of titin in rabbit cardiac-muscle sarcomeres (Linke *et al*., 1999). Here, the technical names of the antibodies (T12, I17, I18, I20/22, MIR) were replaced for simplicity by numbers 1 to 5, with 1 being closest to the Z-disk and 5 being located at the A-band/I-band junction (see Figure 2A). For each antibody type, the epitope-mobility data obtained over a range of SLs from 1.8 to 2.8 μm was pooled in SL bins of 50 nm. For each SL bin, the extension of a given titin segment was measured as the distance flanked by two nearest antibody epitopes: proximal Ig region, epitope 1 to epitope 2; N2B unique sequence, 2 to 3; PEVK, 3 to 4; distal Ig region, 4 to 5. Titin segment extension was then plotted against SL. The corresponding stretch force, F, was determined from mechanical recordings of the (steady-state) PT of isolated rabbit cardiac myofibrils (Linke, 2000).

AFM of engineered titin polyproteins

Single-molecule AFM has been described elsewhere (e.g., Carrion-Vazquez *et al*., 2000; Fisher *et al*., 2000). The cantilevers of the force-measuring unit are standard Si_3N_4 cantilevers from Digital Instruments, Santa Barbara, CA (spring constant, 100 mN/m) or TM Microscopes, Sunnyvale, CA (spring constant, 12 mN/m). Cantilevers were calibrated in solution using the equipartition theorem. AFM experiments described in this study used cloned polyproteins containing either eight identical titin-Ig domains, $I27_8$ (Carrion-Vazquez *et al*., 1999) or I27 domains interspersed with cardiac PEVK-domains, $(I27\text{-}PEVK)_3$ (Li *et al*., 2001) or a construct of the type ($I27_3$-N2B-$I27_3$) (Li *et al*., 2002), where N2B is the 572-residue human cardiac N2B unique sequence. Engineering of these polyproteins has been described in detail (Carrion-Vazquez *et al*., 2000; Li *et al*., 2000, 2001). We note that I27 refers to the original nomenclature of titin domains proposed by Labeit and Kolmerer (1995). Following the discovery of additional Ig-domains in the human gene sequence of titin, the numbering of I27 was changed to I91 (Freiburg *et al*., 2000; Bang *et al*., 2001). In a typical AFM stretch experiment, 3–10 μl of protein sample concentrated at 10–100 μg/ml were deposited onto freshly evaporated gold coverslips, and the protein was allowed to adsorb onto the gold surface. Force–extension measurements were carried out in PBS buffer at an ionic strength of 200–300 mM.

Monte Carlo simulations

The time course of stress relaxation after quick stretch of cardiac myofibrils was reproduced by a Monte Carlo (MC) technique based on entropic elasticity theory (WLC model) and the kinetic parameters of titin-Ig domain unfolding/refolding obtained in AFM stretch experiments with single polyproteins (Carrion-Vazquez *et al*., 1999). Details of the MC approach used by us were described previously (Rief *et al*., 1998). The WLC model of entropic elasticity (Bustamante *et al*., 1994; Marko and Siggia, 1995) predicts the relationship between the relative extension of a polymer (z/L) and the entropic restoring force (f) through

$$f = \left(\frac{k_B T}{A}\right)\left[\frac{1}{4(1 - z/L)^2} - \frac{1}{4} + \frac{z}{L}\right] \quad (1)$$

where k_B is the Boltzmann constant, T is absolute temperature (300 K), A is the persistence length (a measure of the bending rigidity of the chain), z is the end-to-end length, and L is the chain's contour length.

In these MC simulations, the force decay following a stretch was considered to be due to the unfolding of titin-Ig domains (Minajeva *et al*., 2001). As refolding is not observed in the presence of a force, the kinetics of domain refolding have no impact on the results of the simulation (Oberhauser *et al*., 1998; Carrion-Vazquez *et al*., 1999). However, external force greatly affects domain unfolding. The probability of observing the unfolding of any module P_u was calculated as

$$P_u = (k_u^0 \Delta t)(\exp(f \Delta x_u / k_B T)) \quad (2)$$

where k_u^0 is the Ig-domain unfolding rate at zero force, Δt is the polling interval, f is applied force, and Δx_u is the unfolding distance (Carrion-Vazquez *et al*., 1999). The simulations were performed in a LABVIEW (National Instruments, Austin, TX) software environment. A feature of the custom-written software allowed selection of a desired number of iterations.

Results

Titin and collagen are the main determinants of myocardial stiffness

Within the normal 'working' SL range of the heart (1.7–2.3 μm SL; Allen and Kentish, 1985), two main struc-

tural elements have been identified, which are principally important for the elastic properties of the ventricular wall: titin and collagen (Linke *et al*., 1994). Experimental evidence showed that, when the passive length–tension curves of single isolated cardiac myofibrils are compared to those of intact multicellular cardiac preparations, such as trabeculae or papillary muscles (Figure 1A), the curves are similar up to ~2.2 μm SL (Linke *et al*., 1994). This finding holds true also when it is taken into account that myofibrils occupy only about 50–70% of a cardiomyocyte's cross-sectional area. Furthermore, the passive SL–tension curves of single cardiac myofibrils are readily comparable to those of chemically skinned (demembranated) cardiac cells (Figure 1A; see Weiwad *et al*., 2000), indicating that most or all of the structures responsible for the cell's PT development lie inside the sarcomeres. Thus, it was proposed that, up to ~2.2 μm SL, the dominant factor for myocardial PT is titin, whereas at SL >2.2 μm, the high stiffness of the ventricular wall is caused mainly by collagen (Linke *et al*., 1994). Intermediate filaments, such as desmin, contribute nothing or very little to PT development (Wu *et al*., 2000; Anderson *et al*., 2002).

A comparison of PT between different cardiac preparations must consider that species differ in their expression of cardiac-titin isoforms (Freiburg *et al*., 2000). For example, rat and rabbit heart can be compared, as they express almost exclusively the shortest titin isoform, the N2B variant (Figure 1B). Low-percentage SDS–PAGE performed on left ventricular wall tissue from these species detects only trace amounts of the larger N2BA-isoform, with a tendency for rabbit heart to show a slightly higher incidence/degree of N2BA-titin expression than rat heart. However, the passive SL–tension curves of rat and rabbit cardiac myofibrils are virtually indistinguishable (Linke *et al*., 1996b; and Figure 1A). Thus, in both species, titin determines most of the PT over much of the heart's physiological range of extensions, whereas extracellular elements (collagen) are responsible for the steep increase in PT towards the high end of this range. It is likely that this conclusion can also be extended to many other mammalian species. Below we describe our current view of the molecular mechanisms underlying titin elasticity/viscoelasticity in mammalian heart.

In situ *extensibility of cardiac titin segments*

The functionally elastic I-band segment of cardiac titin contains four distinct extensible regions: proximal Ig-domain region, N2B-unique sequence, PEVK domain, and distal Ig-domain region (Figure 2A). In a previous work (Linke *et al*., 1999), we used titin-specific antibodies against epitopes flanking all four regions (numbered 1–5 in Figure 2A) and measured the stretch-dependent extension of each segment by immunoelectron microscopy and immunofluorescence microscopy on rabbit cardiac sarcomeres. A compilation of these data is presented in Figure 2B, showing titin-segment extension plotted against SL. It appears that each titin segment extends in a nonlinear fashion. Also, Ig-domain regions begin to extend before titin's unique sequences. On the other hand, the PEVK domain already stretches before the N2B-unique sequence starts to extend. A differential segment-extension behavior was recognized previously also for skeletal muscle titin (Gautel and Goulding, 1996; Linke *et al*., 1996b). Why do titin segments exhibit these differences in their extensibility?

Single-molecule AFM of titin polyproteins

This question can be answered by performing mechanical measurements directly on titin's molecular subsegments (Li *et al*., 2002). By combining protein engineering and single-molecule AFM approaches (Carrion-Vazquez *et al*., 2000; Fisher *et al*., 2000), interpretational limitations associated with previous single-molecule mechanical studies on whole proteins or large protein fragments (Kellermayer *et al*., 1997; Tskhovrebova *et al*., 1997) can be overcome. For instance, it is possible to study the mechanical properties of individual Ig-domains contained within the elastic I-band titin segment (Figure 3A). An example is shown in Figure 3B, C: a single titin-Ig domain (here, I27 according to nomenclature by Labeit and Kolmerer, 1995; I91 according to nomenclature by Freiburg *et al*., 2000) from the elastic titin region is expressed and multiplied to obtain a polyprotein containing eight serially linked I27 (=I91) modules, $I27_8$ (Figure 3B). Stretching this polyprotein in the AFM gives a characteristic 'fingerprint' (Figure 3C): (1) the force–extension curve shows a sawtooth pattern, in which each peak corresponds to the unfolding of one Ig module; (2) the unfolding force of each peak is ~200 pN (Li *et al*., 2000); and (3) the peaks are spaced at a constant interval. The increase in contour length of the polyprotein when one Ig domain unfolds can be measured with the WLC model of entropic elasticity (Equation (1)). Fitting this model to each sawtooth peak in the measured force trace reveals that each unfolding event increases the contour length of the polyprotein by 28.1 nm (Figure 3C, red curves). Similar experiments have provided us with important new information about the mechanical stability of several other distal and proximal Ig-domains (Li *et al*., 2002).

N2B unique sequence

A novel approach was used to mechanically study the unique sequences in titin, N2B and PEVK (Li *et al*., 2002). Here, the protein fragment of interest is contained within an engineered polyprotein also containing a certain number of I27 (=I91) Ig domains. In the case of the N2B unique sequence, a heteropolyprotein of the type ($I27_3$-N2B-$I27_3$) was generated (Figure 3D, inset). The characteristic 'fingerprinting' of Ig domains when the polyprotein is stretched in the AFM setup, is then used to distinguish recordings obtained from multiple polyproteins from those obtained from a single

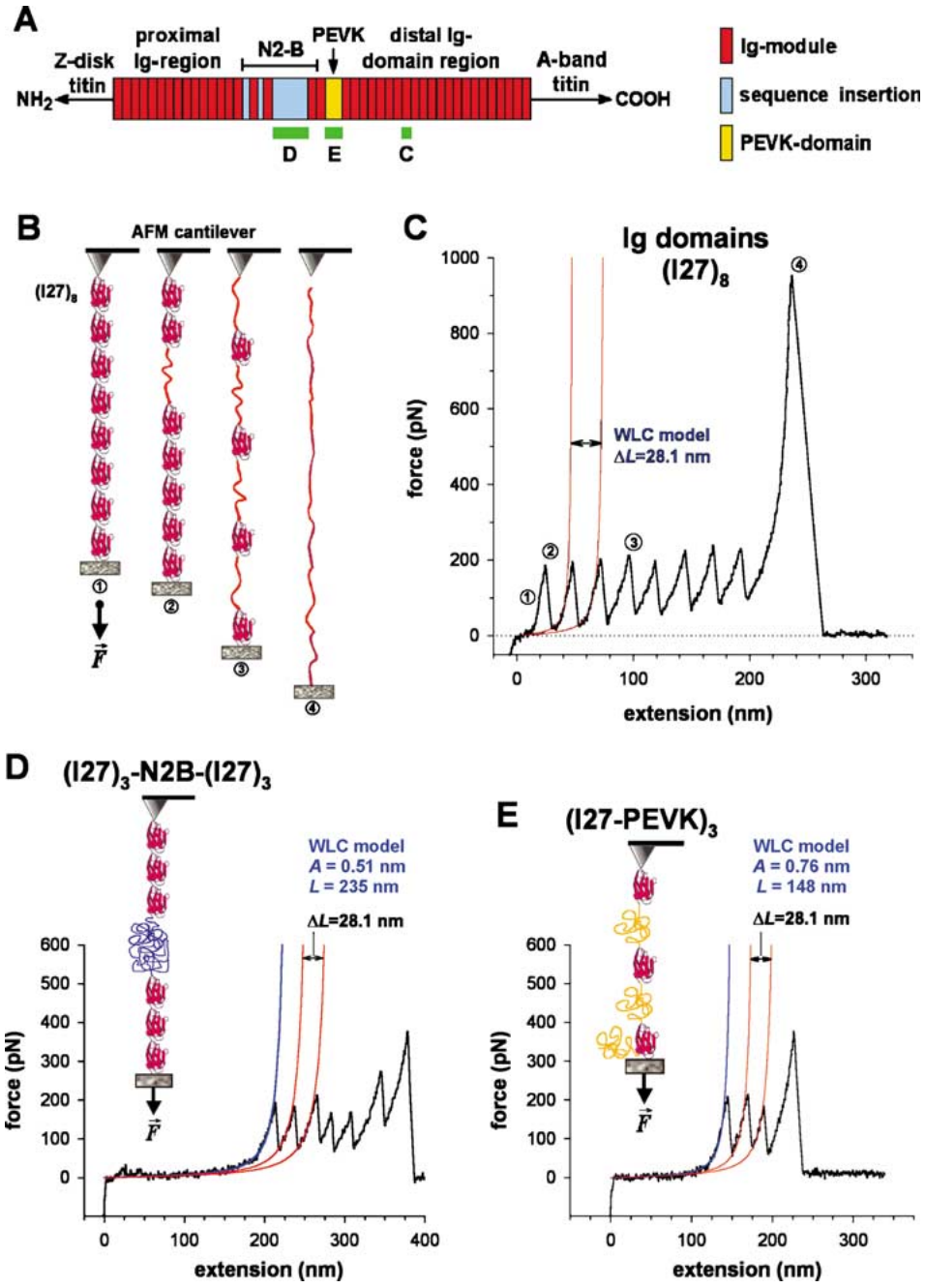

Fig. 3. Single-molecule AFM of engineered titin domains. (A) Domain architecture of the extensible I-band segment of N2B cardiac titin. Thick green bars below scheme indicate location of titin domains studied by AFM; capital letters refer to the panels in this figure showing AFM results for the particular domain. (B) Ig-module I27 (=I91 in nomenclature by Freiburg *et al.*, 2000) can be used as a 'gold standard' in the AFM mechanical measurements of titin domains. Shown is a schematic of how an engineered $I27_8$ (=$I91_8$) polyprotein is attached to the AFM cantilever and a gold-coated coverslip surface and is stretched by a force, *F*. Stages 1–4 correspond to the numbers above the force trace in (C). (C) Typical sawtooth pattern of the force–extension curve of $I27_8$ (=$I91_8$). Force peaks near 200 pN indicate Ig-domain unfolding events. The last peak (4) corresponds to rupture of the polymer from the sites of attachment. The red lines are WLC fits (Levenberg–Marquardt algorithm) based on Equation (1), to the second and third force peak. One unfolding event is calculated to increase the contour length, *L*, of the polyprotein by exactly 28.1 nm. (D) AFM force spectroscopy of a cloned heteropolyprotein consisting of titin's N2B unique sequence flanked by three I27 (=91) Ig domains on either side (Li *et al.*, 2002). The force trace shows a long, featureless, initial region corresponding to N2B extension. The WLC model (Equation (1)) measures the contour length and persistence length of N2B (blue curve). The first six force peaks (near 200 pN) indicate unfolding of all Ig domains within this tether. The spacing between force peaks is a constant 28.1 nm, indicating that a single molecule was stretched. (E) Representative result of AFM studies with engineered polyproteins of the type $(I27\text{-}PEVK)_3$, where 'PEVK' is the 186-residue cardiac PEVK domain of titin's N2B-isoform (Li *et al.*, 2001). Again, the WLC model was used to parameterize PEVK extension (blue curve) and to measure the spacing between Ig-domain unfolding peaks (red curves). Here, the single-molecule tether contained all three I27 Ig modules and two of the three PEVK domains.

polyprotein (for details, see Li *et al.*, 2001, 2002). Only recordings obtained from single polyproteins are included in the statistical analysis. A typical force–extension curve of ($I27_3$-N2B-$I27_3$) is shown in Figure 3D. The

featureless force trace before the first unfolding peak corresponds to the extension of the N2B-unique sequence. In this example, the tether contained all six I27 Ig modules (six unfolding peaks spaced at 28.1 nm) plus the intervening N2B-sequence, which according to WLC calculation (blue curve in Figure 3D) had a contour length, L, of 235 nm. This value is close to the contour length of a fully extended N2B-unique sequence (as expected from the amino-acid sequence; Labeit and Kolmerer, 1995), i.e., the number of residues (572) multiplied by the average, maximally possible, spacing of ~0.4 nm. The average contour length of the N2B-unique sequence, measured from 48 recordings like the one shown in Figure 3D, was 232 nm. The persistence length, A, of the N2B-unique sequence, calculated by the WLC model, was 0.51 nm in the example of Figure 3D and 0.66 nm on average. We found a relatively narrow distribution of persistence lengths, from ~0.4 to 1.3 nm (Li *et al.*, 2002). Thus, it appears that the N2B-unique sequence is a random coil behaving like a purely entropic WLC.

PEVK-domain

Similar AFM experiments were performed with a heteropolyprotein of the type $(I27\text{-}PEVK)_3$ (Li *et al.*, 2001, 2002). The PEVK-domains contained within this construct (Figure 3E, inset) have a length of 186 nm (=PEVK domain of the cardiac N2B isoform; Freiburg *et al.*, 2000) and are interspersed with Ig I27 (=I91) domains to be used for 'fingerprinting'. Again, only recordings obtained from single polyproteins are included in the statistical analysis. Figure 3E shows a typical force–extension curve of $(I27\text{-}PEVK)_3$. No obvious features could be detected in the force trace before the first unfolding peak, which corresponds to the extension of PEVK-titin. The tether contained three I27 Ig modules (three unfolding peaks spaced at 28.1 nm) and two PEVK-domains, as judged from the contour length, $L = 148$ nm, calculated with the WLC model (blue curve in Figure 3E); half this value equals the expected contour length of a fully extended PEVK domain (186 residues times ~0.4 nm). The average contour length of one cardiac PEVK-domain was ~72 nm; the persistence length, A, was 0.76 nm in the example of Figure 3E and 0.91 nm on average (Li *et al.*, 2001, 2002). However, a relatively wide distribution of persistence lengths, from ~0.5 to 2.5 nm, was found. We suggested earlier that this wide range of persistence lengths could be due to multiple conformations of the PEVK domain (Li *et al.*, 2001). In any case, the cardiac PEVK domain can be considered a polymer chain exhibiting WLC properties.

Force–extension relationship of titin's unique sequences: A comparison of in situ *measurements and WLC calculations based on AFM data*

How does the extensibility of the N2B and PEVK sequences, measured by AFM on engineered titin constructs, compare to that of the native unique sequences in the intact cardiac-muscle sarcomere? To make this comparison, we first need to obtain the force–extension relationships of these cardiac-titin segments *in situ*. The (SL-dependent) extension of PEVK and N2B is taken from the plot in Figure 2B (symbols and fits). The stretch force corresponding to a given *in situ* extension is inferred from passive-force measurements on isolated rabbit cardiac myofibrils. Here, we take the purely elastic force component recorded under steady-state conditions, i.e., 2–3 min following a stretch to a new SL. The PT–SL curve used for this purpose is shown in Figure 1A (large symbols with error bars and fit labelled 'rabbit cardiac myofibrils'). These data explicitely do not include viscous and viscoelastic force components. The values of the measured PT are then scaled down to the level of the single titin molecule by assuming a value of 6×10^9 titins per mm^2 cross-sectional area (Li *et al.*, 2002). We also assume that, at a given SL, the (scaled-down) force measured at the ends of the myofibril equals the force acting on each elastic titin segment. This is a reasonable assumption, given that the individual segments in a titin molecule are connected in series and should experience the same stretch force at any time.

Combining the results of titin-segment extensibility studies and myofibrillar force measurements, we can now plot the *in situ* force–extension relationships of both the PEVK-domain and the N2B-unique sequence (Figure 4, symbols and error estimates). Then, we try to reproduce the force corresponding to a given extension (Figure 4, curves) by applying the WLC model of entropic elasticity (Equation (1)). Note that this is not a fitting procedure, but a comparison of measured and calculated data. However, for the calculations we use parameters established experimentally in atomic force spectroscopy measurements (Figure 3; and Li *et al.*, 2002). The end-to-end length (=extension), z, of each region is taken from the fit curves in Figure 2B.

N2B extensibility

To reproduce the force–extension relationship of the N2B-unique sequence, we feed the WLC model with the parameters $L = 230$ nm and $A = 0.66$ nm. Using these parameters, a striking correlation is seen between measured (Figure 4A, symbols and error estimates) and calculated data (Figure 4A, thick curve), at least for forces up to ~6 pN. Values of $A = 0.33$ nm or $A = 1.32$ nm clearly were insufficient to reproduce the *in situ* data (Figure 4A, thin curves). At forces >6 pN, the scatter in the measured data was high, and useful conclusions could not be drawn. Nevertheless, over much of the extension range studied, *in situ* data and AFM-derived reconstitutions gave identical results. For comparison, at physiologically relevant degrees of extension, the equilibrium (elastic) force per titin molecule may reach no more than 3–4 pN (Li *et al.*, 2002). This fact should be kept in mind when interpreting the graphs in Figures 4 and 5.

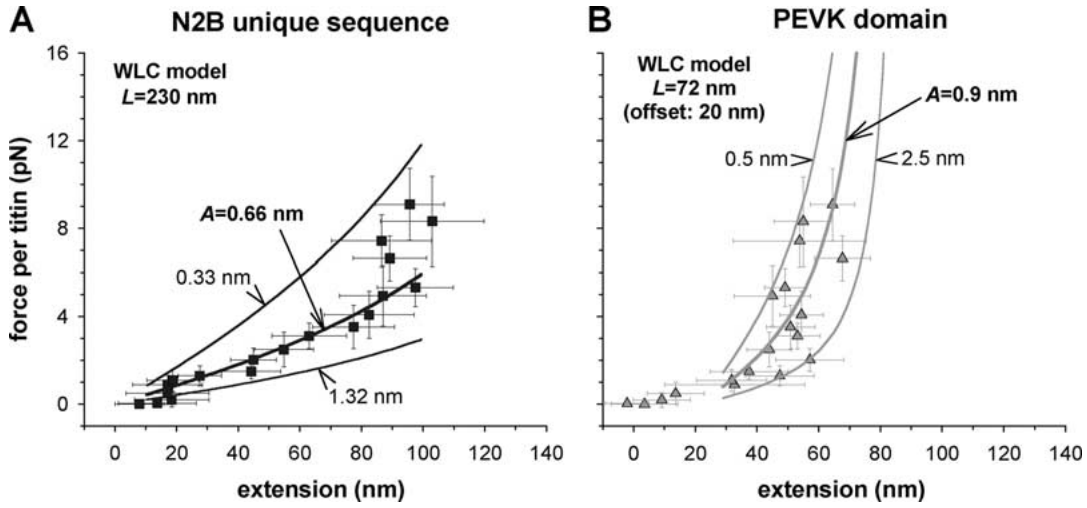

Fig. 4. Reconstitution of the *in situ* force–extension relationships of cardiac titin's unique sequences, based on results obtained in single-molecule AFM measurements. (A) Force-extension data for the N2B-unique sequence of rabbit cardiac sarcomeres (symbols: mean values and error bars). The lines are force–extension curves calculated with the WLC model (Equation (1)), which was fed with a fixed contour length of 230 nm and different persistence lengths (0.66; 0.33; and 1.32 nm). $A = 0.66$ nm produced best results. (B) Force-extension data for the PEVK-domain *in situ* (symbols: mean values and error bars). Lines are force–extension curves calculated with the WLC model (Equation (1)), which was fed with the parameters for persistence length (average: 0.9 nm; upper and lower extremes: 0.5 and 2.5 nm) and contour length (72 nm) established by AFM work. An offset of 20 nm was added to all extension values of these WLC curves, to account for the fact that the antibody epitopes 3 and 4 (Figure 2A) do not directly flank the PEVK-domain. For further details, see text.

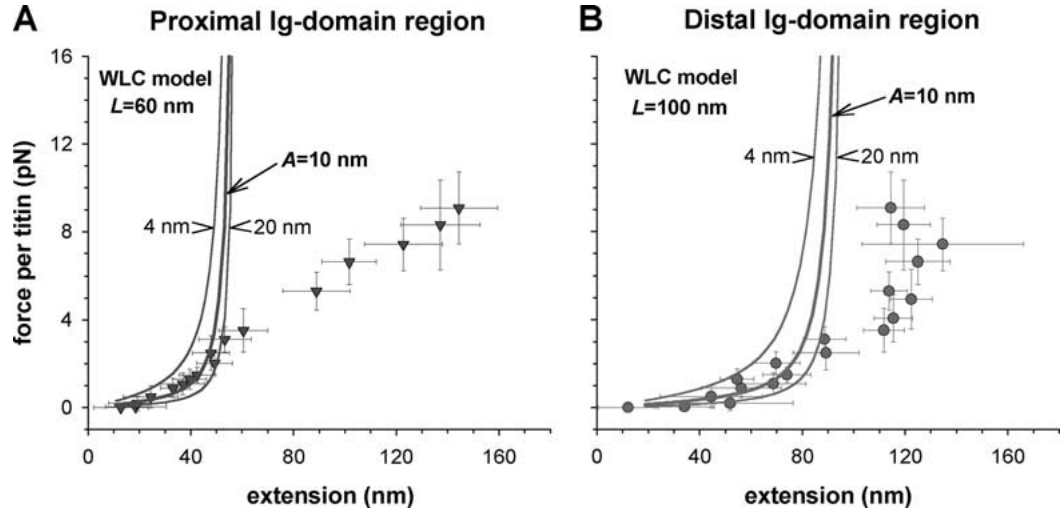

Fig. 5. Comparison of force–extension relationships of Ig-domain regions measured in cardiac sarcomeres with those obtained by WLC modelling. (A) Proximal tandem-Ig region; (B) Distal tandem-Ig-region. *In situ* data (symbols and error bars) were compared to WLC curves (lines) calculated using the indicated parameters for persistence length (A) and contour length (L). Note that physiological stretch forces may not exceed 3–4 pN per titin molecule (Li *et al.*, 2002). For further details, see text.

PEVK extensibility

A description of the PEVK force–extension relationship again uses the parameters previously established for the PEVK-domain in the AFM work: $A = 0.9$ nm and $L = 72$ nm. The thick line in Figure 4B shows that the WLC fit based on these parameters connects the majority of the data points. However, some data points deviate significantly from the modeled curve, especially at forces >4 pN. Using a persistence-length value of 0.5 nm in the WLC model (at constant L) leads to a better description of the high-force data, whereas with $A = 2.5$ nm, reproducibility of measured data is low (Figure 4B, thin lines). However, all data points measured *in situ* fall in between the WLC fit curves obtained with the lowest ($A = 0.5$ nm) and the highest ($A = 2.5$ nm) persistence-length value. Altogether, reconstituting the *in situ* force–extension relationship from AFM results appeared to be feasible.

WLC modelling of in situ *force–extension relationships of Ig-domain regions*

We also try to reproduce the force–extension behavior of the proximal and distal tandem-Ig regions (Figure 5, symbols and error estimates) by using the WLC model. Unfortunately, it is not possible to reliably determine

contour-length and persistence-length values for (relatively short) Ig-domain regions with folded Ig modules by single-molecule AFM force spectroscopy (Li *et al.*, 2002). However, the persistence length, A, of an engineered titin construct containing 12 serially linked tandem-Ig modules ($I27_{12}$) was recently measured on electron microscopic images, and was found to be 10 nm (Li *et al.*, 2002). This is similar to values suggested earlier for whole titin (15 nm, Higuchi *et al.*, 1993; or 13.5 nm, Tskhovrebova and Trinick, 2001). We therefore use $A = 10$ nm as a standard in the WLC calculations. Furthermore, the contour length, L, of the proximal tandem-Ig region was taken to be 60 nm, because the region contains 15 tandem-Ig modules (Labeit and Kolmerer, 1995) and one Ig-module spans approximately 4–4.5 nm (Improta *et al.*, 1996). Corresponding values for the distal Ig-domain region were $L = 100$ nm (22 modules). As before, the fit curves in Figure 2B provide the end-to-end length (or extension), z, of each Ig-domain region.

Proximal Ig-region

Using the above values, we find a good correlation between measured and calculated data describing the proximal Ig-segment extension (Figure 5A), up to forces of ~3 pN per titin molecule. At higher forces, the WLC curve continues to rise steeply, whereas the measured force shows a breakpoint and then increases much more shallow. A clear deviation between measured and calculated data is obvious at forces ≥3.5 pN. This deviation most likely is related to an increased probability of unfolding of individual Ig domains, which is not taken into account in the WLC modelling. The correlation between measured and calculated data was not satisfactory when we used persistence-length values of 4 or 20 nm in the WLC model (Figure 5A, thin curves). In contrast, the good reproducibility of the low-force–extension data, using $A = 10$ nm, suggests that the proximal Ig-domain region (with folded modules) may behave as a purely entropic spring up to an extension of ~45 nm.

Distal Ig-region

Here it was difficult to decide which persistence-length value used in the WLC modelling resulted in best reproducibility of the measured data (Figure 5B). With $A = 10$ nm, the majority of data points up to forces of 2–3 pN could be connected (thick curve), but given the substantial scatter in the measured force–extension data, also the WLC curves using $A = 4$ nm or $A = 20$ nm (thin curves) crossed some points. The measured data clearly deviated from those calculated with the WLC model, at forces ≥3.5 pN. However, no obvious 'breakpoint' could be observed, unlike for the proximal Ig-domain region, and there was no levelling off of the measured force–extension relationship even at high forces. Thus, the graph suggests that unfolding of modules is rather unlikely to occur in the distal Ig-domain region.

Is titin involved in determining viscoelastic properties of cardiac myofibrils?

The analyses described above probed the steady-state (equilibrium) elastic properties of nonactivated cardiac myofibrils. However, if the myofibrils are stretched within the 'working' SL range at physiological stretch rates, they exhibit viscoelastic behavior (Figure 6A). This behavior manifests itself in hysteresis during a stretch-release cycle (Linke *et al.*, 1996a) and in stress relaxation (force decay at constant SL). The magnitude of the stress-relaxation response varies with the stretch rate (Bartoo *et al.*, 1997). Also SL is important: at longer SL, the force-decay amplitude is higher, and stress relaxation lasts longer, than at shorter SL (Figure 6A). In the present study, we asked whether the stretch velocity-sensitive force components could be related to some properties of the titin filaments.

Because PEVK and N2B behave like purely entropic springs (Figure 3), any contribution of titin to myofibrillar viscoelasticity must come from the other extensible titin segments, the Ig-domain regions. In particular, viscoelastic behavior could be due to Ig-domain unfolding. Therefore, our approach was to try to reproduce the force response of cardiac myofibrils to a stretch-hold protocol (Figure 6A) with a MC simulation that takes into account the entropic elasticity of titin regions (Equation (1)), but also the unfolding characteristics of Ig domains established by single-molecule AFM work (Li *et al.*, 2002). This kind of simulation has been attempted previously for skeletal myofibrils (Minajeva *et al.*, 2001). A fresh look into this issue is warranted considering the newly acquired information on the mechanical properties of proximal and distal Ig-domains of cardiac titin (Li *et al.*, 2002). For instance, the unfolding rate at zero force, k_u^0, of the mechanically weakest Ig domain characterized so far by AFM work, is $\sim 3.3 \times 10^{-3}$ s^{-1} (the I4 domain of the proximal tandem-Ig segment). This value is an order of magnitude higher than the previously reported value for I27 (=I91) from the distal Ig-segment (Carrion-Vazquez *et al.*, 1999). In the MC simulations presented here, we generally use $k_u^0 = 3.3 \times 10^{-3}$ s^{-1} to calculate the unfolding probability of an Ig domain, P_u (Equation (2)).

The modeling also considers the presence of the unique sequences in I-band titin, which are modelled as WLC springs with a combined contour length of 300 nm (PEVK = 70 nm; N2B = 230 nm) and a persistence length of 0.9 nm (Li *et al.*, 2002). A fixed value in the simulation is the number of Ig domains within the extensible section of one titin molecule, which is 40 in the N2B-isoform of cardiac titin (Freiburg *et al.*, 2000). For unfolding distance, we use a value of 0.25 nm (Carrion-Vazquez *et al.*, 1999) and for the contour-length gain upon unfolding of one Ig domain, 28.5 nm.

Stress relaxation and Ig-domain unfolding

Figure 6B shows simulated force traces. The stretch amplitudes were 100 nm in both step 1 and step 2, thus

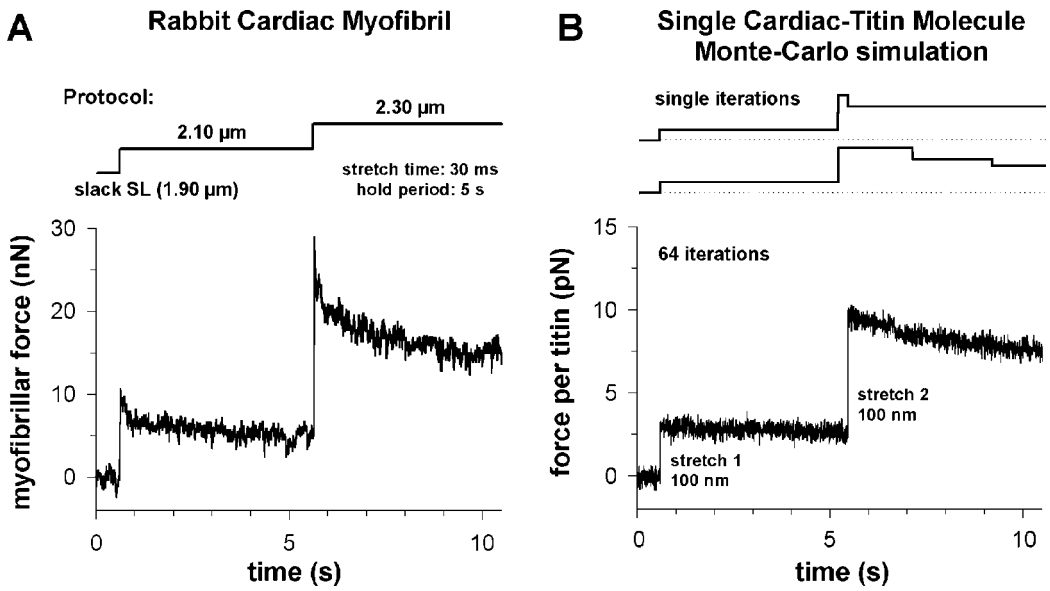

Fig. 6. Stress relaxation of cardiac titin: data measured *in situ* and simulated results using a MC approach. (A) Force response of a small bundle of nonactivated cardiac myofibrils to a stretch-hold protocol of the type shown above the panel. SL is indicated. The force trace is an average of the forces recorded in four consecutive recordings on the same specimen, using the same stretch protocol. (B) MC simulation of 'stress relaxation' of cardiac titin, using Equations (1) and (2), and parameters indicated in the main text. The top traces show two examples of single iterations where both stretch 1 and stretch 2 are 100 nm and each hold period is 5 s. Steps in the second hold period indicate unfolding of titin-Ig domains. The bottom graph shows an average of 64 iterations, to which white noise was added. Note that force relaxation exhibits a similar time course as the slow component of force relaxation in (A).

reproducing the amount of stretch imposed onto I-band titin in sarcomeres extended by $\Delta SL = 0.2$ µm from 1.9 and 2.1 µm SL, respectively (Figure 6A, 'Protocol'). The average force of 64 iterations was calculated, and noise was added to the force trace to make it look more 'real' (Figure 6B). Evidently, the simulated trace does not show strong similarity with the myofibril data. No fast components of force relaxation can be seen in the simulations. However, it appears that the slow components of force relaxation are quantitatively similar in Figure 6A and B. Thus, by feeding the MC simulation with parameters established experimentally in AFM work, part of the stress-relaxation response of cardiac myofibrils is explainable. The results suggest that titin Ig-domain unfolding could underlie the slow component of myofibrillar stress relaxation.

In situ *Ig domain unfolding is a relatively rare event*

To predict how many Ig domains can potentially unfold during stress relaxation, we generated 100 single iterations like the two examples shown in Figure 6B, top. In each iteration, we counted the number of unfolding events, detected as distinct force steps during hold periods. The MC simulation predicted that, over a 5-s-long hold period following a 100 nm/titin step from slack length (simulating a 1.90–2.10 µm SL increase), 0.29 Ig domains per titin molecule unfold on average. Following the second 100 nm/titin step (simulating a 2.10–2.30 µm SL increase), 1.36 Ig domains/titin were predicted to unfold. If the hold time was shortened to 0.5 s (of course, cardiomyocytes *in situ* are not held for long in the stretched state), the values changed to 0.04 (first step-hold) and 0.17 (second step-hold) unfolded Ig domains/molecule. Further, if the hold time was 0.5 s and the step size was modelled to be 200 nm (one step only) – mimicking a more physiological range of motion, from 1.9 to 2.3 µm SL – the MC simulations predicted unfolding of 0.21 Ig domains per titin. Thus, Ig-module unfolding (in the proximal tandem-Ig segment) may become relevant for the viscoelastic behavior of heart muscle when cardiac sarcomeres are stretched to greater physiological SLs.

Fast components of myofibrillar stress relaxation originate in actin–titin interactions

If the fast components of stress relaxation are not due to titin itself (Figure 6), what other factors could be responsible? Recently, we showed that a main determinant of the rapidly decaying viscous force following quick stretch of nonactivated cardiac myofibrils is actin–titin interactions (Kulke *et al.*, 2001a). Isolated rabbit cardiomyofibrils were quickly stretched (within 4 ms) in relaxing buffer from 2.1 to 2.3 µm SL, held in the stretched state, and stress relaxation was measured over a 10-s-long hold period (Figure 7A, left panel). We recorded peak force, as well as steady-state force at the end of the hold period (Figure 7A, panel 'control'). The force decline could be fitted with a three-order exponential-decay function, with decay time constants of 4–5 s, 50–60 ms, and ~30 s (Kulke *et al.*, 2001a). Then, the force decay after stretch was studied in relaxed myofibrils exposed to a Ca^{2+}-independent gelsolin fragment to extract actin. Thin filaments are rapidly removed by gelsolin, except the portion attached to titin in a ~100-nm-wide region adjoining the Z-disk (Linke

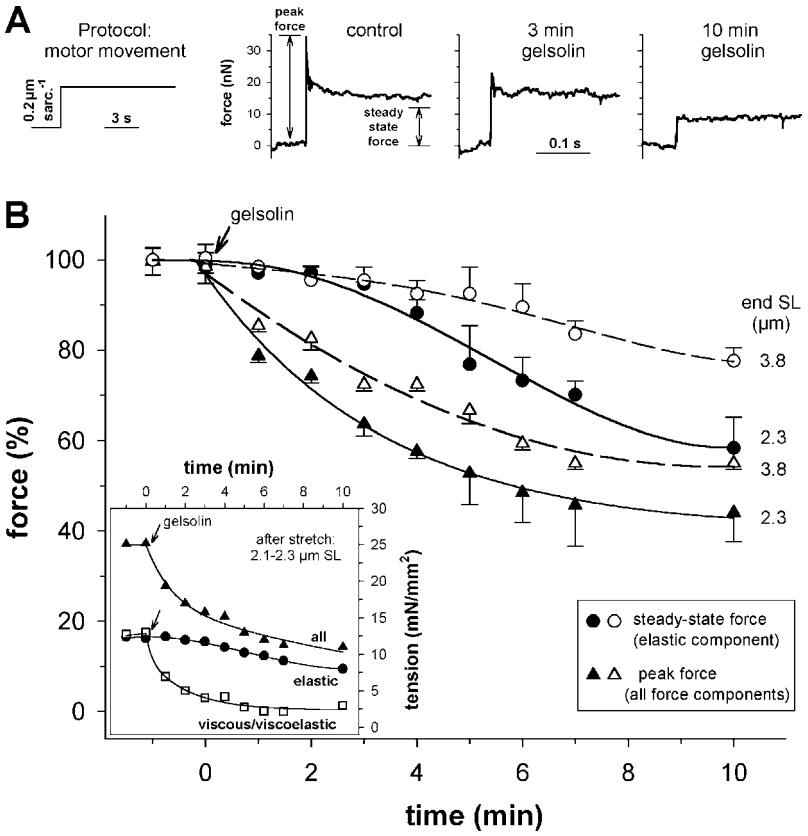

Fig. 7. Stress-relaxation measurements of nonactivated rabbit cardiac myofibrils before and during actin extraction using a Ca^{2+}-independent gelsolin fragment. (A) Motor stretch-hold ramp (stretch completed within 4 ms) and force responses: before actin extraction ('control'), 3 min, and 10 min, respectively, following application of gelsolin. Calibration bar ('0.1 s') applies to all force traces. Note that peak force is greatly decreased after 3-min gelsolin treatment, due to a major drop in the rapidly decaying viscous force component. (B) Comparison of summarized results of stress-relaxation measurements following 4-ms stretches from 2.1 to 2.3 µm SL (filled symbols) or from 3.6 to 3.8 µm SL (open symbols). Data are mean ± SD (n = 6 myofibrils). Curves are third-order regressions (fits to circles) or simple exponential decay functions (fits to triangles). Inset: Example showing absolute force changes related to myofibrillar cross-sectional area. Viscous/viscoelastic force is peak force ('all') minus steady-state force ('elastic').

et al., 1997). Analysis of stress relaxation during gelsolin treatment showed a drop in peak-force amplitude by ~35% within ~3 min (Figure 7A; 7B, filled triangles). During that time period, the velocity-sensitive force components could decrease by as much as 70% (example in Figure 7B, inset, open squares) – attributable almost exclusively to a decrease of the quickly decaying force component (Kulke *et al.*, 2001a). The slower-decay components and steady-state force were affected only >3 min following gelsolin application (Figure 7A, B). Some viscous/viscoelastic force decay remained after 10 min of gelsolin exposure (Figure 7B, inset), and most likely is due to Ig-domain unfolding. However, the results clearly suggest that interactions involving actin and titin play a main role for myofibrillar viscosity.

This conclusion was verified in several control experiments (Kulke *et al.*, 2001a). Most importantly, we tested whether weakly binding crossbridges in the actin–myosin overlap zone might contribute to the stretch-velocity-sensitive forces. Nonactivated cardiac myofibrils were stretched to zero overlap of actin and myosin filaments (3.6 µm SL), and the stretch-hold protocol again was applied before and during actin extraction. Figure 7B shows that results (open symbols) were qualitatively similar to those obtained at shorter SLs (closed symbols). Three minutes of gelsolin treatment decreased peak force by 26–28%, slightly less than the ~35% seen at short SLs. Thus, actin–myosin interactions may contribute to some degree to viscous force decay following quick stretch of relaxed muscle. However, most of the viscous drag originates in actin–titin interactions. Earlier, we have provided evidence that the only elastic I-band-titin region involved in (weak) binding to actin, is the PEVK-domain (Kulke *et al.*, 2001a; Linke *et al.*, 2002).

Discussion

The issues addressed in this study concern the molecular basis of (visco)elasticity in normal myocardium. Based on the results shown, the following questions will be discussed:

(1) How significant is titin, particularly in comparison to collagen, in determining the overall stiffness of the heart in diastole?

(2) What are the molecular mechanisms of elasticity of the individual titin regions that together, provide the

sarcomere with a unique passive length–tension relationship? How and why do the four distinct extensible titin regions differ in their (steady-state) elastic properties?
(3) Do cardiac titin filaments, or interactions involving the elastic titin segment, play a role in determining velocity-sensitive (viscous, viscoelastic) passive force components in myofibrils?

(1) Titin and collagen stiffness in myocardium

Compared to other proteins with known elastic function, cardiac titin was estimated to have a stiffness similar to that of elastin (Urry, 1984), but much lower than collagen (Linke *et al*., 1994). In rabbit cardiac sarcomeres, predominant expression of the short N2B-titin leads to PT levels >10 times higher than those measured (at the same SL) in psoas-muscle sarcomeres expressing the longer N2A-titin isoform (Linke *et al*., 1994; Kulke *et al*., 2001b). Conversely, vertebrate cardiac N2B-titin is about an order of magnitude less stiff than the titin-like proteins present in the I-bands of *Drosophila* indirect flight muscle (Kulke *et al*., 2001b).

The observation that single rabbit cardiac myofibrils and multicellular cardiac preparations generate about the same passive force per unit cross-sectional area, over much of the physiological SL range of myocardium (approximately 1.7–2.3 μm; Allen and Kentish, 1985), led to a model describing the role of titin and collagen in mammalian heart (Linke *et al*., 1994). Accordingly, the myofibrillar titin-filament system is responsible for most of the diastolic stiffness of the whole heart at extensions corresponding to ≤2.2 μm SL. The extracellular collagen network becomes more important than titin in determining the PT level (wall stiffness), only at long physiological SLs above ~2.2 μm (Linke *et al*., 1994). Here, we provided an updated account of our results relevant to this topic (Figure 1). Furthermore, passive force per unit cross-sectional area is independent of the presence of desmin – as found in mechanical measurements on skinned muscle fibers of desmin knockout mice (Anderson *et al*., 2002) – and intermediate filaments are thus unlikely to make a significant contribution to passive stiffness. Similar conclusions have been drawn by others (Wu *et al*., 2000). Both titin elasticity (Neagoe *et al*., 2002) and collagen stiffness (Weber, 1997) can be altered in pathological situations, but it is the increased fibrosis and hence, the dramatic rise in collagen content, which mainly causes the much-elevated end-diastolic pressure levels in failing hearts (Neagoe *et al*., 2002; Hein *et al*., 2002). Nevertheless, titin can be considered the main determinant of myocardial passive stiffness in normal healthy hearts.

(2) Molecular basis of cardiac-titin elasticity

Recently we showed that the steady-state (equilibrium) force–extension relationship of nonactivated cardiac myofibrils can be fully reconstituted with a mathematical model that is fed with parameters determined in single-molecule AFM measurements on engineered titin domains (Li *et al*., 2002). In the present study, we functionally 'dissected' the elastic I-band titin (cardiac N2B isoform) into its four structurally distinct regions (Figure 2) and constructed a force–extension curve for each region (*in situ*) by using previously established experimental data (Linke *et al*., 1999). We then tested whether the regions can be described as purely entropic springs behaving accoding to WLC theory (Figures 4, 5). We found that within the physiological SL range, all four regions may indeed exhibit entropic elasticity. However, there are important differences in the mechanical behavior of these regions, which are highlighted below.

Ig-domain regions: At low stretch forces, titin's tandem-Ig-regions straighten out (Erickson, 1994), thus being responsible for most of the extensibility of sarcomeres at shorter physiological lengths (Linke *et al*., 1996b). The Ig-regions essentially are semiflexible polymer chains with a low contour-length to persistence–length ratio of 6:1 to 10:1 (Figure 5). Polymer-elasticity theory predicts that little force is needed for the initial extension (straightening) of such polymer chains; they behave more like a leash than a spring (Erickson, 1997).

At higher stretch forces (>4 pN/titin molecule), the proximal Ig-domain region is more 'stretchable' than the distal Ig-region (Figure 5; also see Gautel *et al*., 1996, and Linke *et al*., 1999). Li *et al*. (2002) showed that a main difference between the two tandem-Ig-regions is that the proximal Ig-domains have dramatically higher unfolding probabilities than the distal Ig-domains. The distal Ig-domain region seems to be designed to avoid unfolding of its modules – a property that could be important for the proposed interaction between parallel titin strands in that region (Liversage *et al*., 2001). In contrast, the proximal Ig-domain region clearly must unfold some of its modules to reach the extensions measured in highly extended cardiac sarcomeres (Linke *et al*., 1996a). In conclusion, both Ig-domain regions act mainly as entropic springs, but it cannot be ruled out that Ig-domain unfolding in the proximal region contributes to the mechanical behavior of cardiac titin *in situ*. However, Ig-domain unfolding is energy-costly and thus, massive unfolding may not be part of the normal mechanism of titin elasticity. On the other hand, already the unfolding of only one Ig-domain per titin molecule drops force by a great amount (Minajeva *et al*., 2001). Thus, by (reversibly) unfolding just a few modules, titin's proximal Ig-region can act as a 'shock absorber' to prevent damaging high stretch forces acting on a muscle.

Unique sequences: Both the N2B-PEVK domain and the N2B-unique sequence of cardiac titin behave as entropic WLCs *in vitro* (Figure 3) and apparently *in situ* (Figure 4). If these titin regions are indeed random coils, as proposed (Li *et al*., 2002), none of them should be involved in contour-length adjustments of titin in the cardiac sarcomere (Helmes *et al*., 1999). Whether PEVK-elasticity generally is purely entropic or also

has an enthalpic component, is not entirely clear. Enthalpic contributions to (mainly) entropic elasticity were proposed earlier for skeletal PEVK-titin (Linke *et al*., 1998a; Gutierrez-Cruz *et al*., 2001). Differences in elastic properties between skeletal and cardiac PEVK-titins may be expected, due to differences in the modular structure of these domains (Greaser, 2001). We note that the PEVK-domain of N2B-cardiac titin studied here by AFM, in fact is constitutively expressed in all muscle types (Freiburg *et al*., 2000). The conclusions reached in the present work may therefore extend to the C-terminal portion of the PEVK sequences of all titin isoforms (Linke *et al*., 2002). In sum, titin's unique sequences can be viewed in principle as entropic springs, but some modulatory role might be played by 'enthalpic' elasticity mechanisms.

To explain why significant extension of the N2B-unique sequence begins only at longer SLs (Linke *et al*., 1999), WLC elasticity theory can be used: the force needed to extend a WLC is higher, the greater the chain's ratio between contour length and persistence length. The *L*:*A* ratio measured for titin's N2B-unique sequence, is 232:0.66, or ~350:1 (Li *et al*., 2002). In comparison, the *L*:*A* ratio determined for the cardiac PEVK-domain, is 72:0.91, or ~80:1. Therefore, the PEVK-domain will extend at lower forces than the N2B-unique sequence. Even lower forces are needed to extend (straighten) titin's tandem-Ig regions (*L*:*A* ratio, 6:1 to 10:1). These considerations provide a theoretical explanation for the differential extension of the four distinct cardiac-titin regions under equilibrium forces.

Finally, it remains to be seen, whether the thermal fluctuations of the entropic titin spring could be constrained significantly in the environment of the sarcomeric filament lattice. Some evidence suggesting that there is little constraint imposed on the Brownian motion of titin, comes from the observation that the steady-state elasticity of relaxed muscle fibers is not influenced by the presence of 4% dextran in the bathing medium (Ranatunga, 2001). As dextran shrinks the lattice spacing (Konhilas *et al*., 2002), an effect on (equilibrium) elasticity of myofibrils would have been expected if steric hindrance of titin fluctuations were increased.

(3) Cardiac titin and myofibrillar viscoelasticity

If the mechanical properties of cardiac-titin regions were based entirely on entropic mechanisms, the force development upon stretch of titin should not exhibit any dependency on stretch velocity. However, when nonactivated single myofibrils are stretched at different rates, PT shows stretch velocity-sensitive components (Bartoo *et al*., 1997; Minajeva *et al*., 2001). This kind of viscous/viscoelastic behavior is seen also in intact or demembranated muscle fibers (de Tombe and ter Keurs, 1992; Wang *et al*., 1993; Mutungi and Ranatunga, 1996, 1998). Until some time ago, the viscoelasticity of muscle had been attributed largely to the presence of weak interactions between actin and myosin filaments (weakly bound crossbridges; Hill, 1968; Proske and Morgan, 1999). A re-evaluation of this earlier concept became necessary with the general acceptance of titin as a principal passive force-bearing element in the sarcomere. In a previous study, we showed that unfolding of a relatively small number of titin-Ig-domains is sufficient to explain a significant portion of the viscoelastic force decay following stretch of skeletal myofibrils (Minajeva *et al*., 2001). Here, using new data accumulated in mechanical studies on both cardiac-titin domains and isolated cardiac myofibrils, we made a prediction as to whether or not titin filaments play a role for the stretch velocity-sensitive passive-force components in cardiac muscle.

Results of MC simulations indicated that some viscoelastic force decay of stretched cardiac myofibrils might be due to unfolding of a minor fraction of proximal titin-Ig domains (Figure 6). Importantly, Ig-domain unfolding could explain only the slow phases of stress relaxation, but not the rapidly decaying forces. We caution that the evidence for a contribution of titin domains to slow viscoelastic force decay is only indirect. However, our evidence is based on real, measured AFM data on the unfolding probability of the mechanically weakest proximal Ig-module in cardiac titin (Li *et al*., 2002). Similarly, in the MC approach, we specifically excluded that unique sequences in titin make a contribution to stress relaxation (PEVK and N2B were modelled as pure WLCs) – an assumption made based on the results of AFM force spectroscopy. In any case, the fact that slow stress relaxation is still seen in thin filament-extracted cardiac myofibrils containing only Z-disks, titin, and thick filaments (Figure 7B, inset), led us to argue that structural rearrangements within titin itself contribute to viscoelasticity of sarcomeres.

Mechanical measurements on actin-extracted cardiac myofibrils revealed that a large portion of the viscous/viscoelastic force decay – mainly the quickly decaying component – originates in actin–titin interactions (Figure 7; and Kulke *et al*., 2001a). We estimated that approximately 80% of the stress relaxation following rapid stretch could be due to weak actin–titin binding, the remainder resulting from interactions between actin and myosin filaments (Figure 7B). Thus, weakly bound crossbridges could make a small contribution to passive muscle properties (Campbell and Lakie, 1998; Proske and Morgan, 1999), but much of the viscoelasticity is unrelated to actin–myosin interactions (Kulke *et al*., 2001a). The fact that actin–titin interactions are the principal source of viscous drag in the sarcomere, was not taken into consideration in a recent calculation aimed at quantifying sarcomeric viscoelasticity (Ranatunga, 2001). Consequently, the values calculated fell short by a factor of at least five, of the experimental values known from mechanical measurements on relaxed muscle fibers (Mutungi and Ranatunga, 1996, 1998). We suggest that actin–titin interactions account for most, if not all, of the heretofore unexplained viscous effects.

Novel twists in titin viscoelasticity: By far not all elastic titin regions interact with the thin filaments. Besides a 100-nm-wide (functionally stiff) titin segment adjoining the Z-disk (Linke *et al*., 1997; Trombitas *et al*., 1997), the only I-band-titin domain found to bind to actin, is the PEVK domain (Kulke *et al*., 2001a). Furthermore, the actin-PEVK titin interaction was shown to be modulated by Ca^{2+} (Kulke *et al*., 2001a), which might give rise to lowered viscous drag. Future studies will focus on the exciting possibility that titin's viscoelastic properties can be adjusted *in situ* by regulatory mechanisms involving the action of Ca^{2+} ions (Stuyvers *et al*., 1998) and/or other, still unknown, factors (Linke *et al*., 2002).

Acknowledgements

We thank all members of the Linke and Fernandez laboratories for their important contributions to the works cited in this article. We acknowledge financial support of the Deutsche Forschungsgemeinschaft (grants Li 690/2-3 and Li 690/6-2). W.A.L. is supported by a Heisenberg fellowship from the Deutsche Forschungsgemeinschaft.

References

Allen DG and Kentish JC (1985) The cellular basis of the length–tension relation in cardiac muscle. *J Mol Cell Cardiol* **17:** 821–840.

Alper J (2002) Protein structure. Stretching the limits. *Science* **297:** 329–331.

Anderson J, Joumaa V, Stevens L, Neagoe C, Li Z, Mounier Y, Linke WA and Goubel F (2002) Passive stiffness changes in soleus muscles from desmin knockout mice are not due to titin modifications. *Pflügers Arch* **444:** 771–776.

Bang ML, Centner T, Fornoff F, Geach AJ, Gotthardt M, McNabb M, Witt CC, Labeit D, Gregorio CC, Granzier H and Labeit S (2001) The complete gene sequence of titin, expression of an unusual approximately 700-kDa titin isoform, and its interaction with obscurin identify a novel Z-line to I-band linking system. *Circ Res* **89:** 1065–1072.

Bartoo ML, Linke WA and Pollack GH (1997) Basis of passive tension and stiffness in isolated rabbit myofibrils. *Am J Physiol* **273:** C266–C276.

Bustamante C, Marko JF, Siggia ED and Smith S (1994) Entropic elasticity of λ-phage DNA. *Science* **265:** 1599–1600.

Campbell KS and Lakie M (1998) A cross-bridge mechanism can explain the thixotropic short-range elastic component of relaxed frog skeletal muscle. *J Physiol* **510:** 941–962.

Carrion-Vazquez M, Oberhauser AF, Fowler SB, Marszalek PE, Broedel SE, Clarke J and Fernandez JM (1999) Mechanical and chemical unfolding of a single protein: a comparison. *Proc Natl Acad Sci USA* **96:** 3694–3699.

Carrion-Vazquez M, Oberhauser AF, Fisher TE, Marszalek PE, Li H and Fernandez JM (2000) Mechanical design of proteins studied by single-molecule force spectroscopy and protein engineering. *Prog Biophys Mol Biol* **74:** 63–91.

Chiu Y-L, Ballou EW and Ford LE (1982) Internal viscoelastic loading in cat papillary muscle. *Biophys J* **40:** 109–120.

de Tombe P and ter Keurs HEDJ (1992) An internal viscous element limits unloaded velocity of sarcomere shortening in rat myocardium. *J Physiol* **454:** 619–642.

Erickson HP (1994) Reversible unfolding of fibronectin type III and immunoglobulin domains provides the structural basis for stretch and elasticity of titin and fibronectin. *Proc Natl Acad Sci USA* **91:** 10,114–10,118.

Erickson HP (1997) Stretching single protein molecules: titin is a weird spring. *Science* **276:** 1090–1092.

Fisher TE, Marszalek PE and Fernandez JM (2000) Stretching single molecules into novel conformations using the atomic force microscope. *Nature Struct Biol* **7:** 719–724.

Freiburg A, Trombitas K, Hell W, Cazorla O, Fougerousse F, Centner T, Kolmerer B, Witt C, Beckmann JS, Gregorio CC, Granzier H and Labeit S (2000) Series of exon-skipping events in the elastic spring region of titin as the structural basis for myofibrillar elastic diversity. *Circ Res* **86:** 1114–1121.

Fürst DO, Osborn M, Nave R and Weber K (1988) The organization of titin filaments in the half-sarcomere revealed by monoclonal antibodies in immunoelectron microscopy: a map of ten nonrepetitive epitopes starting at the Z line extends close to the M line. *J Cell Biol* **106:** 1563–1572.

Gautel M and Goulding D (1996) A molecular map of titin/connectin elasticity reveals two different mechanisms acting in series. *FEBS Lett* **385:** 11–14.

Gautel M, Lehtonen E and Pietruschka F (1996) Assembly of the cardiac I-band region of titin/connectin: expression of the cardiac-specific regions and their structural relation to the elastic segments. *J Muscle Res Cell Motil* **17:** 449–461.

Greaser M (2001) Identification of new repeating motifs in titin. *Proteins* **43:** 145–149.

Gutierrez-Cruz G, van Heerden AH and Wang K (2001) Modular motif, structural folds and affinity profiles of the PEVK segment of human fetal skeletal muscle titin. *J Biol Chem* **276:** 7442–7449.

Hein S, Gaasch WH and Schaper J (2002) Giant molecule titin and myocardial stiffness. *Circulation* **106:** 1302–1304.

Helmes M, Trombitas K, Centner T, Kellermayer M, Labeit S, Linke WA and Granzier H (1999) Mechanically driven contour-length adjustment in rat cardiac titin's unique N2B sequence: titin is an adjustable spring. *Circ Res* **84:** 1339–1352.

Higuchi H, Nakauchi Y, Maruyama K and Fujime S (1993) Characterization of beta-connectin (titin 2) from striated muscle by dynamic light scattering. *Biophys J* **65:** 1906–1915.

Hill DK (1968) Tension due to interaction between the sliding filaments in resting striated muscle. The effect of stimulation. *J Physiol* **199:** 637–684.

Improta S, Politou A and Pastore A (1996) Immunoglobulin-like modules from I-band titin: extensible components of muscle elasticity. *Structure* **4:** 323–337.

Itoh Y, Suzuki T, Kimura S, Ohashi K, Higuchi H, Sawada H, Shimizu T, Shibata M and Maruyama K (1988) Extensible and less-extensible domains of connectin filaments in stretched vertebrate skeletal muscle sarcomeres as detected by immunofluorescence and immunoelectron microscopy using monoclonal antibodies. *J Biochem* **104:** 504–508.

Julian FJ, Sollins MR and Moss RL (1976) Absence of a plateau in length-tension relationship of rabbit papillary muscle when internal shortening is prevented. *Nature* **260:** 340–342.

Kellermayer MSZ, Smith SB, Granzier HL and Bustamante C (1997) Folding-unfolding transitions in single titin molecules characterized with laser tweezers. *Science* **276:** 1112–1116.

Kentish JC, ter Keurs HE, Ricciardi L, Bucx JJ and Noble MI (1986) Comparison between the sarcomere length-force relations of intact and skinned trabeculae from rat right ventricle. Influence of calcium concentrations on these relations. *Circ Res* **58:** 755–768.

Konhilas JP, Irving TC and de Tombe PP (2002) Myofilament calcium sensitivity in skinned rat cardiac trabeculae: role of interfilament spacing. *Circ Res* **90:** 59–65.

Kulke M, Fujita-Becker S, Rostkova E, Neagoe C, Labeit D, Manstein DJ, Gautel M and Linke WA (2001a) Interaction between PEVK-titin and actin filaments: origin of a viscous force component in cardiac myofibrils. *Circ Res* **89:** 874–881.

Kulke M, Neagoe C, Kolmerer B, Minajeva A, Hinssen H, Bullard B and Linke WA (2001b) Kettin, a major source of myofibrillar stiffness in *Drosophila* indirect flight muscle. *J Cell Biol* **154:** 1045–1057.

Labeit S and Kolmerer B (1995) Titins, giant proteins in charge of muscle ultrastructure and elasticity. *Science* **270:** 293–296.

Labeit S, Gautel M, Lakey A and Trinick J (1992) Towards a molecular understanding of titin. *EMBO J* **11:** 1711–1716.

Li H, Linke WA, Oberhauser AF, Carrion-Vazquez M, Kerkvliet JG, Lu H, Marszalek PE and Fernandez JM (2002) Reverse engineering of the giant muscle protein titin. *Nature* **418:** 998–1002.

Li H, Oberhauser AF, Fowler SB, Clarke J and Fernandez JM (2000) Atomic force microscopy reveals the mechanical design of a modular protein. *Proc Natl Acad Sci USA* **97:** 6527–6531.

Li H, Oberhauser AF, Redick SD, Carrion-Vazquez M, Erickson HP and Fernandez JM (2001) Multiple conformations of PEVK proteins detected by single-molecule techniques. *Proc Natl Acad Sci USA* **98:** 10,682–10,686.

Linke WA (2000) Stretching molecular springs: elasticity of titin filaments in vertebrate striated muscle. *Histol Histopathol* **15:** 799–811.

Linke WA, Popov VI and Pollack GH (1994) Passive and active tension in single cardiac myofibrils. *Biophys J* **67:** 782–792.

Linke WA, Bartoo ML, Ivemeyer M and Pollack GH (1996a) Limits of titin extension in single cardiac myofibrils. *J Muscle Res Cell Motil* **17:** 425–438.

Linke WA, Ivemeyer M, Olivieri N, Kolmerer B, Rüegg JC and Labeit S (1996b) Towards a molecular understanding of the elasticity of titin. *J Mol Biol* **261:** 62–71.

Linke WA, Ivemeyer M, Labeit S, Hinssen H, Rüegg JC and Gautel M (1997) Actin-titin interaction in cardiac myofibrils: probing a physiological role. *Biophys J* **73:** 905–919.

Linke WA, Ivemeyer M, Mundel P, Stockmeier MR and Kolmerer B (1998a) Nature of PEVK-titin elasticity in skeletal muscle. *Proc Natl Acad Sci USA* **95:** 8052–8057.

Linke WA, Stockmeier MR, Ivemeyer M, Hosser H and Mundel P (1998b) Characterizing titin's I-band Ig domain region as an entropic spring. *J Cell Sci* **111:** 1567–1574.

Linke WA, Rudy DE, Centner T, Gautel M, Witt C, Labeit S and Gregorio CC (1999) I-band titin in cardiac muscle is a three-element molecular spring and is critical for maintaining thin filament structure. *J Cell Biol* **146:** 631–644.

Linke WA, Kulke M, Li H, Fujita-Becker S, Neagoe C, Manstein DJ, Gautel M and Fernandez JM (2002) PEVK domain of titin: an entropic spring with actin-binding properties. *J Struct Biol* **137:** 194–205.

Liversage AD, Holmes D, Knight PJ, Tskhovrebova L and Trinick J (2001) Titin and the sarcomere symmetry paradox. *J Mol Biol* **305:** 401–409.

Marko JF and Siggia ED (1995) Stretching DNA. *Macromolecules* **28:** 8759–8770.

Maruyama K, Murakami F and Ohashi K (1977) Connectin, an elastic protein of muscle. Comparative Biochemistry. *J Biochem* (*Tokyo*) **82:** 339–345.

Minajeva A, Kulke M, Fernandez JM and Linke WA (2001) Unfolding of titin domains explains the viscoelastic behavior of skeletal myofibrils. *Biophys J* **80:** 1442–1451.

Mutungi G and Ranatunga KW (1996) Tension relaxation after stretch in resting mammalian muscle fibers: stretch activation at physiological temperatures. *Biophys J* **70:** 1432–1438.

Mutungi G and Ranatunga KW (1998) Temperature-dependent changes in the viscoelasticity of intact resting mammalian (rat) fast- and slow-twitch muscle fibres. *J Physiol* **508:** 253–265.

Neagoe C, Kulke M, del Monte F, Gwathmey JK, de Tombe PP, Hajjar R and Linke WA (2002) Titin isoform switch in ischemic human heart disease. *Circulation* **106:** 1333–1341.

Noble MIM (1977) The diastolic viscous properties of cat papillary muscle. *Circ Res* **40:** 288–292.

Oberhauser AF, Marszalek PE, Erickson HP and Fernandez JM (1998) The molecular elasticity of the extracellular matrix protein tenascin. *Nature* **393:** 181–185.

Politou AS, Thomas DJ and Pastore A (1995) The folding and stability of titin immunoglobulin-like modules, with implications for the mechanism of elasticity. *Biophys J* **69:** 2601–2610.

Proske U and Morgan DL (1999) Do cross-bridges contribute to the tension during stretch of passive muscle? *J Muscle Res Cell Motil* **20:** 433–442.

Ranatunga KW (2001) Sarcomeric visco-elasticity of chemically skinned skeletal muscle fibres of the rabbit at rest. *J Muscle Res Cell Motil* **22:** 399–414.

Rief M, Gautel M, Oesterhelt F, Fernandez JM and Gaub HE (1997) Reversible unfolding of individual titin immunoglobulin domains by AFM. *Science* **276:** 1109–1112.

Rief M, Fernandez JM and Gaub HE (1998) Elastically coupled two-level systems as a model for biopolymer extensibility. *Phys Rev Lett* **81:** 4764–4767.

Stuyvers BD, Miura M, Jin JP and ter Keurs HE (1998) Ca^{2+}-dependence of diastolic properties of cardiac sarcomeres: involvement of titin. *Progr Biophys Mol Biol* **69:** 425–443.

Trinick J and Tskhovrebova L (1999) Titin: a molecular control freak. *Trends Cell Biol* **9:** 377–380.

Trombitas K, Greaser ML and Pollack GH (1997) Interaction between titin and thin filaments in intact cardiac muscle. *J Muscle Res Cell Motil* **18:** 345–351.

Tskhovrebova L and Trinick J (2001) Flexibility and extensibility in the titin molecule: analysis of electron microscope data. *J Mol Biol* **310:** 755–771.

Tskhovrebova L, Trinick J, Sleep JA and Simmons RM (1997) Elasticity and unfolding of single molecules of the giant muscle protein titin. *Nature* **387:** 308–312.

Urry DW (1984) Protein elasticity based on conformations of sequential polypeptides: the biological elastic fiber. *J Protein Chem* **3:** 403–436.

Wang K (1996) Titin/connectin and nebulin: giant protein rulers of muscle structure and function. *Adv Biophys* **33:** 123–134.

Wang K, McCarter R, Wright J, Beverly J and Ramirez-Mitchell R (1993) Viscoelasticity of the sarcomere matrix of skeletal muscles. The titin-myosin composite filament is a dual-stage molecular spring. *Biophys J* **64:** 1161–1177.

Weber KT (1997) Extracellular matrix remodeling in heart failure: a role for de novo angiotensin II generation. *Circulation* **96:** 4065–4082.

Weiwad WK, Linke WA and Wussling MH (2000) Sarcomere length-tension relationship of rat cardiac myocytes at lengths greater than optimum. *J Mol Cell Cardiol* **32:** 247–259.

Wu Y, Cazorla O, Labeit D, Labeit S and Granzier H. (2000) Changes in titin and collagen underlie diastolic stiffness diversity of cardiac muscle. *J Mol Cell Cardiol* **32:** 2151–2162.